Check for updates

Development of novel bone targeting peptide–drug conjugate of 13-aminomethyl-15-thiomatrine for osteoporosis therapy†

Jia Su,‡[a] Chao Liu, [ID] ‡[b] Haohao Bai,[b] Wei Cong,[b] Hua Tang,[b] Honggang Hu,[b] Li Su,*[b] Shipeng He [ID] *[b] and Yong Wang*[a]

13-Aminomethyl-15-thiomatrine (**M19**) previously developed by our research group was a promising candidate for novel anti-osteoporosis drug development. However, the application of **M19** was limited by its unsatisfactory druggability including poor chemical stability, excessively broad pharmacological activity and some degree of cytotoxicity. To solve these problems, **M19**-based bone targeting and cathepsin K sensitive peptide–drug conjugates (**BTM19-1**, **BTM19-2** and **BTM19-3**) were developed to realize precise drug release in the bone tissue. Subsequent studies showed a rapid drug release process *via* cathepsin K digestion but sufficient stability over several hours in chymotrypsin. Besides, greatly improved chemical stability and strong hydroxyapatite binding affinity were also demonstrated. In biological evaluation studies, these PDCs showed less cytotoxicity and similar osteoclast inhibitory activity compared with the prototype drug. The optimal **BTM19-2** could serve as a suitable candidate for further osteoporosis therapy research.

Introduction

Osteoporosis, a bone disease characterized by systematic loss of bone mass and deterioration of bone microstructure, affects 200 million people worldwide and causes 1.6 million hip fractures and 7.4 million other fractures every year, and is regarded as a public health problem.[1–3] Nowadays, many drugs have been developed and used clinically for osteoporosis therapy, such as bisphosphonates, selective estrogen receptor modulators, teriparatide and so on, which have already achieved certain efficacy in clinical application. However, there were still some limitations and side effects in long-term use and dose maintenance.[4–6]

Matrine was a quinolizidine alkaloid isolated from the roots of *Sophora flavescens*, *Sophora tonkinensis* and *Sophora alopecuroides* which showed a variety of pharmacological activities including antibacterial, anti-arrhythmia, anti-tumor, anti-fibrosis and anti-inflammatory, *etc*.[7–11] In our previous study, **M19** was developed and represented the new generation of highly active matrine derivative because of its great inhibitory effect on pro-inflammatory cytokine TNF-α and NF-κB

transcriptional activity, making it a promising anti-inflammatory drug candidate.[9] Recently, we showed that **M19** could block NF-κB, AKt, MAPK and other signalling pathways by stabilizing ribosomal protein S5 (RPS5), thereby inhibiting RANKL-induced osteoclast differentiation and alleviating bone loss in ovariectomized mice.[12] However, direct development of **M19** into anti-osteoporosis drug was generally limited. First of all, the excessively broad pharmacological activity of **M19** may bring the risk of off-target effects.[13–15] Besides, the biological particularity of bone tissue, such as high tissue density and poor permeability, brought great difficulties to drug delivery.[16] More importantly, the druggability of **M19** was not satisfactory owing to its poor chemical stability and strong alkalinity. Therefore, novel drug design strategies need to be applied to realize its role as anti-osteoporosis drug.

Peptide–drug conjugates (PDCs), novel prodrug modification strategy, have been widely employed in the development of anti-malignant tumor drugs.[17–21] By covalently coupling functional peptides to drugs with specific linker, PDCs could selectively deliver drugs to target cells/tissues/organs, reducing systemic toxicity and improving pharmacokinetic and pharmacodynamic parameters.[22,23] Inspired by their promising success in targeted cancer therapy, we envisioned that conjugation with bone targeting peptide would make **M19** to have bone-targeting characteristics as well as improve its anti-osteoporosis potency. Herein, **M19**-based bone targeting PDCs were rationally developed by coupling **M19** with bone targeting peptide and cathepsin K sensitive smart linker through suitable spacers. These PDCs showed excellent specificity for hydroxyapatite

[a]Department of Orthopaedics, Wenzhou Hospital of Integrated Traditional Chinese and Western Medicine, Zhejiang, China. E-mail: wyhpi008@163.com

[b]Institute of Translational Medicine, Shanghai University, Shanghai, China. E-mail: suli1020@shu.edu.cn; heshipeng@shu.edu.cn

† Electronic supplementary information (ESI) available. See DOI: 10.1039/d1ra08136e

‡ Jia Su and Chao Liu contributed equally to this work.

(HA), the composition of bone tissue and tooth, and inhibitory activity on osteoclast differentiation, providing a valuable example for overcoming the shortcomings of natural product source compounds and improve their druggability.

Results and discussion

Rational design of M19-based bone targeting PDCs

To rational design bone-targeting PDCs, bone-targeting selective peptides and enzyme sensitive linkers need to be considered. First of all, as a special connective tissue, bone tissue was composed of a variety of cells and intercellular bone matrix with high inorganic salt content which was mainly composed of HA. In previous studies, tetracycline,[24] bisphosphonates,[25] hydroxymalonic acids[26] and small heterocyclic compounds[27] were often used in design of bone targeting drug molecules or drug carriers. In recent years, more and more peptide sequences with excellent bone targeting ability have been found, such as polyaspartic acid (hydroxyapatite targeting),[28] Ser–Asp–Ser–Ser–Asp (osteoblasts specific factor-2 targeting),[29] Ser–Thr–Phe–Thr–Lys–Ser–Pro (hematopoietic stem cell targeting)[30] and (Asp–Ser–Ser)[6] (hydroxyapatite targeting),[31] etc. Compared with bone-targeting small molecules, these peptides have clear mechanism, high targeting affinity and low side effects.[32] Since **M19** has been found excellent inhibitory effect on osteoclasts, rather than promotion effect on osteoblasts, moderate length polyaspartic acids (Asp–Asp–Asp–Asp–Asp–Asp), whose HA binding affinity was comparable to tetracycline and calcein,[28] was chosen as the target peptide sequence for this work.

Secondly, it was reported that osteoclasts effectively degraded extracellular matrix proteins through secretion of cathepsin K, which was a crucial protease for the degradation of bone organic matrix collagen type I and type II and specifically distributed in Howship's lacunae formed by osteoclasts and osteocytes.[33,34] Therefore, peptide sequences sensitive to cathepsin K could be served as cleavable linker of PDCs for drug releasing in bone tissue. At present, some peptide substrates such as GGGMGPSGPWGGK[35] and GHPGGPQGKC[36] have been employed in researches of bone relative material development. However, amino acids would remain on the material after specific degradation which was not suitable for PDCs use. Notably, Bossard and co-workers[37] found that a series of short peptide (1–3 amino acids) were specific substrates of cathepsin K. And among them, the substrate Cbz–Leu–Arg–AMC (AMC, 7-

amino-4-methylcoumarin) could quickly and specifically release AMC under the treatment of cathepsin K with high apparent secondary rate constant, making dipeptide Leu–Arg an ideal cleavable linker in this work.

In addition, in order to increase the overall hydrophilicity of PDCs and avoid steric hindrance, a polyethylene glycol spacer and 1,6-self-immolative *p*-aminobenzyloxycarbonyl (PABC) structure were introduced between the polyaspartic acids, sensitive dipeptide and drug molecule (Fig. 1).
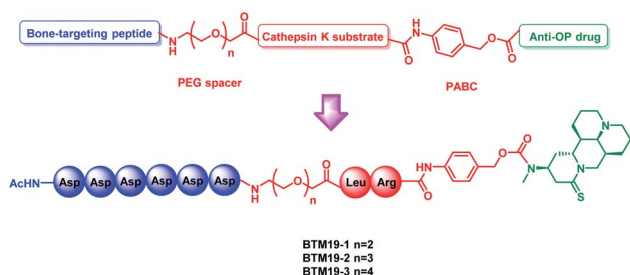
Synthesis of M19-based bone targeting PDCs

To begin with, thiosophocarpine (**2**) was obtained by reacting commercially available sophocarpine (**1**) with Lawesson's reagent in toluene solution. In this step, viscous insoluble by-products generated in the reaction system need to be removed continuously to ensure the smooth progress of the reaction. Subsequent Michael addition reaction between **2** and methylamine provided **M19** in a yield of 65% (Scheme 1A).

With the prototype drug in hand, the next step was the synthesis of on-resin peptide precursors Asp(OtBu)$_6$–PEG$_n$–Leu–Arg(Pbf)–Resin (**3–5**) concluding poly-aspartic acid polypeptide, polyethylene glycol of different lengths and leucine–arginine sequence through standard SPPS process using [[(6-chloro-1H-benzotriazol-1-yl)oxy](dimethylamino)-N,N-dimethylmethani-
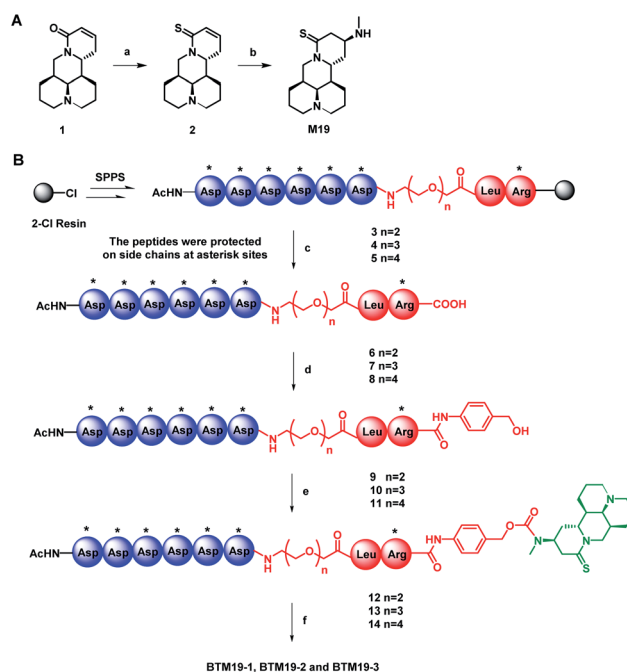
Scheme 1 The synthesis route of **M19** (A) and PDCs (B). Reagents and conditions: (a) Lawesson's reagent, toluene, reflux, 2 h, 37%; (b) methylamine ethanol solution, rt, 12 h, 65%; (c) TFE/DCM (1 : 3, v/v), rt, 4 h, 80–83%; (d) 4-aminophenyl methanol, HOBt, DIC, DMF, rt, 2 h, 74–79%; (e) (i) triphosgene, activated carbon, THF, rt, 12 h; (ii) **M19**, Et$_3$N, DMF, rt, 12 h, 78–86% in two steps; (f) TFA/water/EDT/TIPs (95 : 2 : 2 : 1, v/v/v/v), rt, 2 h, 60–63%. The resin-bound peptides were protected on side chains at asterisk sites: *tert*-butyl (*t*Bu; for Asp) and (2,2,4,6,7-pentamethyl-2,3-dihydro-1-benzofuran-5-yl)sulfonyl (Pbf; for Arg).

Fig. 1 General design of the novel **M19**-based bone targeting PDCs. PEG = polyethylene glycol; PABC = *p*-aminobenzyloxycar-bonyl.

minium hexafluorophosphate (HCTU) and N,N-diisopropylethyl-amine (DIPEA) as coupling reagents. After cleavage from the resin with trifluoroethanol, full protected intermediates Asp(OtBu)$_6$–PEG$_n$–Leu–Arg(Pbf) (**6–8**) were coupled with 4-aminobenzyl alcohol by $1H$-1,2,3-benzotriazole (HOBt) and N,N'-diisopropylcarbodiimide to construct 1,6-self-immolative p-amino-benzyloxycarbonyl (PABC) linker containing intermediates Asp(OtBu)$_6$–PEG$_n$–Leu–Arg(Pbf)–PABC (**9–11**). The following reaction between **9–11** with triphosgene and **M19** in the presence of DIPEA given protected PDCs Asp(OtBu)$_6$–PEG$_n$–Leu–Arg(Pbf)–PABC–**M19** (**12–14**). Finally, global deprotection of compounds **12–14** with K reagent obtained the target PDCs (**BTM19-1**, **BTM19-2** and **BTM19-3**). Pure products were obtained as a freeze-dried powder with a good chemical yield of 59–63% after purification by preparative reverse phase chromatography and subsequent lyophilization (Scheme 1B).

Chemical stability studies of M19-based bone targeting PDCs

In our previous research, we found that the chemical stability of **M19** was unsatisfactory. It spontaneously converted to thiosophocarpine through retro-Michael reaction in the solution at room temperature. Therefore, we firstly conducted chemical stability investigation of the synthesized PDCs (Fig. 2A and ESI Fig. S1†). **M19** and **BTM19-1**, **BTM19-2** and **BTM19-3** were dissolved in water/MeCN solutions and incubated for 14 days at room temperature respectively. As shown in Fig. 2A, **M19** decomposed into thiosophocarpine as anticipation with a half-life of 1.7 days. While PDCs were relatively stable within 14 days' incubation without any significant degradation. It suggested that, benefitting from PDCs construction, the chemical stability of prototype drug **M19** was greatly improved. One possible explanation was that the newly generated amide bond structure

stabilized the lone pair of the 13-position aminomethyl group *via* electron withdrawing conjugate.

Drug release properties of M19-based bone targeting PDCs with cathepsin K

According to our design, the bone targeting PDCs should release **M19** under conditions prevailing around osteoclasts by the cathepsin K digestion and following degradation of 1,6-self-immolative PABC linker. Besides, the pH optimum of cathepsin K was documented to be pH 5.5 depending on the nature of the substrate.[38] Thus, we investigated the drug release properties in an acidic system to simulate the Howship's lacunae in bones (Fig. 2B and ESI Fig. S2†). As shown in Fig. 2B, under the specific conditions (cathepsin K 5 nM, 100 mM Na acetate at pH 5.5 containing 20 mM cysteine and 5 mM EDTA), both prodrugs were cleavaged and released prototype **M19**. The half-life was 54 minutes for **BTM19-1**, 48 minutes for **BTM19-2** and 51 minutes for **BTM19-3** and all the PDCs could be completely cleavaged after 240 minutes' treatment.

Enzymatic stability studies of M19-based bone targeting PDCs

The protease stability was an important criterion for biological activity of synthesized PDCs, which ensured the transportation of active cargo to the target cell, tissue and/or organ.[39] To determine their hydrolytic enzymes tolerance, **BTM19-1**, **BTM19-2** and **BTM19-3** were incubated with chymotrypsin at 37 °C and analysed by HPLC (Fig. 2C and ESI Fig. S3†). It was found that the cathepsin K cleavable PDCs were stable under these conditions with no **M19** or other degradation products observed after 240 minutes' exposure.

Hydroxyapatite binding affinity of M19-based bone targeting PDCs

Subsequently, we assessed the affinity between the novel bone targeting PDCs and the bone mineral HA. Fifteen equivalents of HA were incubated with **BTM19-1**, **BTM19-2** and **BTM19-3** at 37 °C and pH 5.5 to simulate the acidic circumstance in the Howship's lacunae. As shown in Fig. 2D and S4 (ESI†), approximately 50% of both PDCs were bound to hydroxyapatite after 20 minutes' treatment and it reached over 95% after 80 minutes. In order to have a more comprehensive understanding, the negative control **BTM19-4** with a scrambled peptide sequence was successfully realized (ESI Scheme S1†). When **BTM19-4** was incubated with HA powder under the same condition, only very weak binding could be observed after 80 minutes' incubation. These results suggested that the high affinity between **M19** based PDCs with HA was generated from the polyaspartic acid moiety rather than **M19** itself.

Cytotoxicity of M19-based bone targeting PDCs

In previous studies, **M19** performed a certain degree of cytotoxicity, especially to liver cells. Thus, CCK-8 analysis was performed on RAW264.7 cells to test their potential toxicity (ESI Fig. S5†). The results showed that the prototype drug **M19** exhibited about 20% cell viability inhibition at concentration of
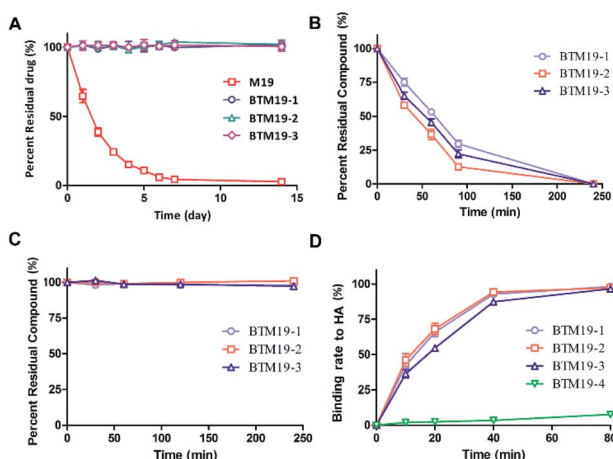

Fig. 2 (A) Quantitative data of chemical stability study of **M19** *vs.* PDCs in water/MeCN solution at rt; (B) quantitative data of drug release study of PDCs at pH 5.5 and 37 °C with cathepsin K; (C) quantitative data of proteolytic stability study of PDCs under a-chymotrypsin treatment C; (D) quantitative data of binding study of PDCs with hydroxyapatite at pH = 5.5 and 37 °C; data points were displayed as the mean value SEM of duplicate independent experiments.

10 μM, while little significant cytotoxicity at a concentration range of 1–10 μM was observed for all PDCs, indicated that the introduction of the bone-targeting moiety reduced the toxicity of the prototype drug, enlightening us that the cytotoxicity of **M19** may originated from 13-position aminomethyl group, especially related to its alkalinity.

In vitro osteoclast inhibition activity of M19-based bone targeting PDCs

The next move was to evaluate their biological activity against RANKL-induced osteoclast differentiation on RAW264.7 cells *via* tartrate-resistant acid phosphatase (TRAP) staining (Fig. 3 and ESI Fig. S6†). Different concentrations of PDCs and **M19** were co-cultured with RANKL and colony stimulating factor 1 (CSF-1) in RAW264.7 cells. After 3 days' treatment, both compounds exhibited dose-dependently inhibitory effects on the TRAP activity and the IC_{50} was 2.41 μM (**M19**), 4.38 μM (**BTM19-1**), 2.62 μM (**BTM19-2**) and 2.84 μM (**BTM19-3**). These results indicated that, with the exception of **BTM19-1**, the osteoclast suppression effect produced by the **M19**-based PDCs was equivalent to that of the free **M19**, confirming the bone-targeted PDC modification strategy did not significantly affect the activity of the prototype drug. However, **BTM19-1** exhibited a heavily decreased activity. A reasonable speculation might be

that the steric hindrance caused by its shorter PEG linker prevented cathepsin K from substrates cleaving, which delayed the release of the prototype drug.

Experimental

General methods

Materials and instruments. Fmoc-protected amino acids were commercially available from GL Biochem (Shanghai) Ltd. Other reagents and solvents were brought from Acros, Sigma-Aldrich, Alfa Aesar, Sinopharm Chemical Reagent Co., Ltd. and Innochem Chemical Reagent. Dichloromethane (DCM) was distilled over calcium hydride (CaH_2) or NaH under argon atmosphere. All reactions vessels were oven-dried before use. Reactions were monitored by thin-layer chromatography (TLC) and visualized by UV analyzer (254 nm). ^{1}H and ^{13}C-NMR spectra was recorded on a Bruker 600 MHz instrument. Chemical shifts (δ) were reported relative to TMS (0 ppm) for ^{1}H-NMR and ^{13}C-NMR spectra. The coupling constants (J) were displayed in Hertz (Hz) and the splitting patterns were defined as follows: singlet (s); broad singlet (s, br); doublet (d); doublet of doublet (dd); triplet (t); quartet (q); multiplet (m). ESI-MS was measured with a Bruker Esquire-LC mass spectrometer. High resolution mass (HR-MS) spectra were measured on a Waters Xevo G2 QTOF mass spectrometer.

Peptide synthesis and characterization. Peptide synthesis vessels were self-made. DIPEA, HOBt, HCTU, DIC, and 2-chlorotritylchloride resin were purchased from GL Biochem (Shanghai) Ltd. The crude peptides were dissolved with CH_3CN/H_2O and analysed or purified by analytical or semi-preparative RP-HPLC, respectively. A Vydac C_4 or C_{18} column (5 μm, 4.6 mm × 250 mm) with a 1 mL min^{-1} flow rate was used for analytical RP-HPLC, and a Vydac C4 column (10 μm, 10 mm × 250 mm or 22 mm × 150 mm) with a 3–6 mL min^{-1} flow rate was used for semi-preparative RP-HPLC. The solvents systems were buffer A (0.1% TFA in water), buffer B (0.1% TFA in CH_3CN). Data were recorded and analysed using the software system LC Solution.

15-Thiosophocarpine (2). To a solution of sophocarpine (**1**, 9.8 g, 40 mmol) in toluene was slowly added Lawson's reagent (8.0 g, 20 mmol). The reaction mixture was refluxed for 2 hours. The solvent was concentrated and the residue was purified by column chromatography (50 : 1–10 : 1, DCM/MeOH) to afford **2** as a yellow powder (3.9 g, 37%). ^{1}H-NMR (600 MHz, CDCl$_3$): δ 6.47–6.46 (m, 1H), 6.08–6.05 (m, 1H), 5.09 (dd, J = 6 Hz, J = 18 Hz, 1H), 4.33 (s, 1H), 3.03 (s, 1H), 2.92 (s, 2H), 2.68–2.64 (m, 1H), 2.36–2.31 (m, 2H), 2.05 (s, 3H), 1.85–1.80 (m, 3H), 1.72–1.69 (m, 1H), 1.63–1.55 (m, 1H), 1.50–1.42 (m, 3H); ^{13}C-NMR (600 MHz, CDCl$_3$): δ 189.76, 131.95, 127.59, 63.77, 57.01, 54.34, 50.79, 39.96, 34.92, 27.47, 26.55, 24.96, 20.89, 20.35; ESI-MS m/z calculated for $C_{15}H_{22}N_2S$ 262.15; found $[M + H]^+$ = 263.2.

13-Aminomethyl-15-thiomatrine (M19, 3). **2** (3.9 g, 15 mmol) was added in methylamino alcohol solution (10 mL, 90 mmol). The reaction mixture was stirred for 12 hours at room temperature. The solvent was concentrated and the residue was purified by column chromatography (50 : 1–10 : 1, DCM/MeOH) to afford **3** as a yellow powder (2.9 g, 65%). ^{1}H-NMR (600 MHz,
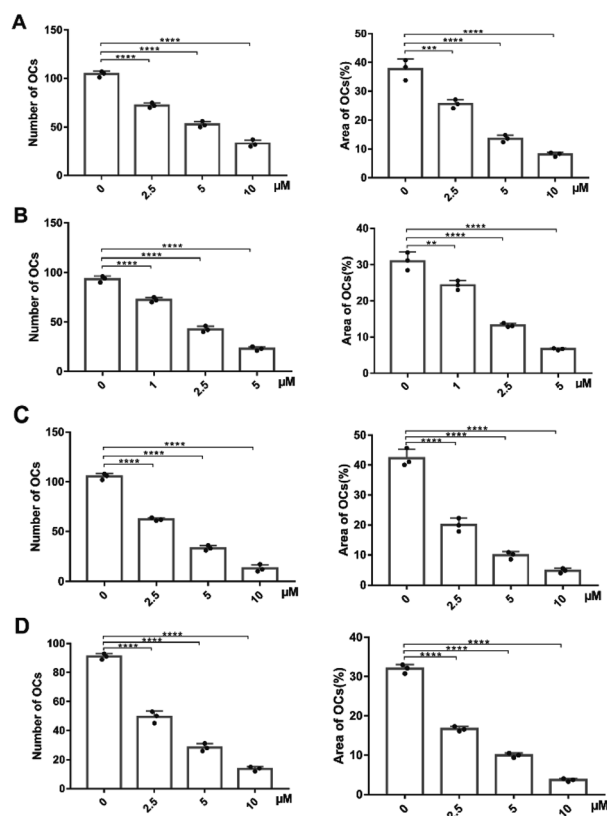

Fig. 3 Quantitative data of TRAP-positive cells formation from RAW264.7 cells with the treatment of **M19** (A), **BTM19-1** (B), **BTM19-2** (C) and **BTM19-3** (D) respectively based on numbers (left) and area (right) (*P < 0.05, **P < 0.01, ***P < 0.001, ****P < 0.0001).

CDCl$_3$): δ 5.43 (dd, $J = 6$ Hz, $J = 12$ Hz, 1H), 4.26–4.24 (m, 1H), 3.52 (t, $J = 12$ Hz, 1H), 3.24–3.21 (m, 1H), 2.97–2.92 (m, 1H), 2.88–2.80 (m, 3H), 2.24 (s, 3H), 2.17 (s, 1H), 2.04–1.98 (m, 2H), 1.94–1.88 (m, 4H), 1.74–1.71 (m, 2H), 1.64–1.61 (m, 2H), 1.59–1.55 (m, 2H), 1.48–1.44 (m, 3H); ^{13}C-NMR (600 MHz, CDCl$_3$): δ 195.46, 63.55, 56.98, 56.96, 55.58, 50.90, 49.39, 47.91, 42.69, 35.63, 33.64, 30.38, 27.63, 26.56, 21.12, 20.59; ESI-MS m/z calculated for C$_{16}$H$_{27}$N$_3$S 293.19; found [M + H]$^+$ = 294.2.

Asp(OtBu)$_6$–PEG$_n$–Leu–Arg(Pbf)–resin (3–5 and 15). The 2-chlorotritylchloride resin (1 g, loading capacity = 1 mmol g^{-1}, 1% DVB, 100–200 mesh) was swollen in DCM/DMF mixture solvent for 10 minutes. After pre-activation of 4 equivalents of Fmoc-protected amino acid in DMF for 5 minutes using 3.8 equivalents of HCTU and 8 equivalents of DIPEA, the solution was added to the resin. After 50 minutes, the resin was washed (5× DMF, 5× DCM, 5× DMF) to provide on resin peptide 3–5 and 15.

Asp(OtBu)$_6$–PEG$_n$–Leu–Arg(Pbf) (6–8 and 15). The cleavage cocktail (TFE/DCM = 1 : 3, v/v) was added to the resin at room temperature. After stirring for 2 hours, the cleavage cocktail was collected and concentrated. The chilled diethyl ether was added to the concentrated residue to precipitate the crude peptides. The peptide suspensions were centrifuged for 3 minutes at 3000 rpm and then the clear solution was decanted to afford 6–8 and 15.

6 as a white powder (1.43 g, 82%). HR-MS m/z calculated for C$_{81}$H$_{132}$N$_{12}$O$_{28}$S 1752.8995; found [M + 2H]$^{2+}$ = 877.4609.

7 as a white powder (1.5 g, 83%). HR-MS m/z calculated for C$_{83}$H$_{136}$N$_{12}$O$_{29}$S 1796.9257; found [M + 2H]$^{2+}$ = 899.4961.

8 as a white powder (1.47 g, 80%). HR-MS m/z calculated for C$_{85}$H$_{140}$N$_{12}$O$_{30}$S 1840.9519; found [M + 2H]$^{2+}$ = 921.4898.

16 as a white powder (1.6 g, 87%). HR-MS m/z calculated for C$_{90}$H$_{150}$N$_{14}$O$_{24}$S 1843.0668; found [M + 2H]$^{2+}$ = 922.5041.

Asp(OtBu)$_6$–PEG$_n$–Leu–Arg(Pbf)–PABC (9–11 and 16). To a solution of Asp(OtBu)$_6$–PEG$_n$–Leu–Arg(Pbf)–PABC and HOBt (1.5 equivalents) in DMF was added DIC (3 equivalents). The reaction was stirred at room temperature for 15 minutes and then the 4-aminobenzyl was added. The mixture was stirred for 12 hours at room temperature. The solvent was removed and the residue was re-solved in EA and successively washed with 1 M HCl (3 × 100 mL) and brine (3 × 100 mL), dried over Na$_2$SO$_4$, filtered and concentrated. The chilled diethyl ether was added to the concentrated residue to precipitate the crude peptides. The peptide suspensions were centrifuged for 3 minutes at 3000 rpm and then the clear solution was decanted to obtain 9–11 and 16.

9 as a white powder (1.12 g, 79%). HR-MS m/z calculated for C$_{88}$H$_{139}$N$_{13}$O$_{28}$S 1857.9573; found [M + 2H]$^{2+}$ = 929.9841.

10 as a white powder (1.18 g, 75%). HR-MS m/z calculated for C$_{90}$H$_{143}$N$_{13}$O$_{29}$S 1901.9835; found [M + 2H]$^{2+}$ = 951.9905.

11 as a white powder (1.15 g, 74%). HR-MS m/z calculated for C$_{92}$H$_{147}$N$_{13}$O$_{30}$S 1946.0098; found [M + 2H]$^{2+}$ = 974.0215.

16 as a white powder (125 g, 74%). HR-MS m/z calculated for C$_{97}$H$_{157}$N$_{15}$O$_{24}$S 1948.1247; found [M + 2H]$^{2+}$ = 975.0709.

Asp(OtBu)$_6$–PEG$_n$–Leu–Arg(Pbf)–PABC–M19 (12–14 and 17). To a solution of bis(trichloromethyl)carbonate (1.1 equivalents) in THF was added activated carbon (catalytic amount). The reaction mixture was stirred vigorously at room temperature for 30 minutes and then, Asp(OtBu)$_6$–PEG$_n$–Leu–Arg(Pbf)–PABC was added. After overnight stirring, the activated carbon was filtered and the filtrate was concentrated. The residue was re-dissolved in DMF, Et$_3$N (3 equivalents) and a solution of **M19** in DMF was added dropwise at 0 °C. The mixture was stirred at room temperature overnight. The reaction mixture was diluted with EA and water, and the organic phase was separated, washed with brine (3 × 100 mL), dried over Na$_2$SO$_4$, filtered and concentrated. The chilled diethyl ether was added to the concentrated residue to precipitate the crude peptides. The peptide suspensions were centrifuged for 3 minutes at 3000 rpm and then the clear solution was decanted to provide **12–14** and **17**.

12 as a white powder (1.1 g, 78%). HR-MS m/z calculated for C$_{105}$H$_{164}$N$_{16}$O$_{29}$S$_2$ 2177.1292; found [M + 2H]$^{2+}$ = 1089.5528.

13 as a white powder (1.07 g, 85%). HR-MS m/z calculated for C$_{107}$H$_{168}$N$_{16}$O$_{30}$S$_2$ 2221.1554; found [M + 2H]$^{2+}$ = 1111.5709.

14 as a white powder (1.09 g, 86%). HR-MS m/z calculated for C$_{109}$H$_{172}$N$_{16}$O$_{31}$S$_2$ 2265.1816; found [M + 2H]$^{2+}$ = 1133.5828.

17 as a white powder (1.05 g, 76%). HR-MS m/z calculated for C$_{114}$H$_{182}$N$_{18}$O$_{25}$S$_2$ 2267.2965; found [M + 3H]$^{3+}$ = 756.7441.

Asp$_6$–PEG$_n$–Leu–Arg–PABC–M19 (BTM19-1, BTM19-2, BTM19-3 and BTM19-4). The cleavage cocktail (TFA/TIPS/EDT/water = 95 : 2 : 2 : 1, v/v/v/v) was added to the Asp(OtBu)$_6$–PEG$_n$–Leu–Arg(Pbf)–PABC–**M19** at room temperature. After stirring for 2 hours, the solvent was concentrated. The chilled diethyl ether was added to the concentrated residue to precipitate the crude peptides. The peptide suspensions were centrifuged for 3 minutes at 3000 rpm and then the clear solution was decanted. The resulting white residues were dissolved in MeCN/H$_2$O, analysed by HPLC and HR-MS and purified by RP-HPLC to afford **BTM19-1**, **BTM19-2**, **BTM19-3** and **BTM19-4**.

BTM19-1 as a white powder (492 mg, 62%). HR-MS m/z calculated for C$_{68}$H$_{100}$N$_{16}$O$_{26}$S 1588.6715; found [M + H]$^+$ = 1589.6329.

BTM19-2 as a white powder (493 mg, 63%). HR-MS m/z calculated for C$_{70}$H$_{104}$N$_{16}$O$_{27}$S 1632.9678; found [M + 2H]$^{2+}$ = 817.4979.

BTM19-3 as a white powder (443 mg, 60%). HR-MS m/z calculated for C$_{72}$H$_{108}$N$_{16}$O$_{28}$S 1676.7240; found [M + 2H]$^{2+}$ = 839.3631.

BTM19-4 as a white powder (458 mg, 59%). HR-MS m/z calculated for C$_{80}$H$_{126}$N$_{18}$O$_{20}$S 1690.9116; found [M + 2H]$^{2+}$ = 846.4346.

Chemical stability studies

To investigate the degradation rates, **BTM19-1**, **BTM19-2**, **BTM19-3** and **M19** were dissolved in water/MeCN solution (9 : 1, v/v, 0.1 mg mL^{-1}) and stirred at room temperature respectively. The percentage of residue was monitored by HPLC at 0, 1, 2, 3, 4, 5, 6, 7 and 14 days.

Drug release studies

820 mg sodium acetate, 242 mg cysteine and 146 mg EDTA were dissolved in 100 mL PBS buffer solution and adjusted pH = 5.5

to afford buffer solution. 10 μL of 0.5 mg mL^{-1} cathepsin K active human solution was diluted 2000 times for later use. 1 μM **BTM19-1**, **BTM19-2** and **BTM19-3** were respectively dissolved with 1 mL buffer solution and then diluted 10 times for later use. 100 μL of cathepsin K solution and PDCs solution was mixed and incubated in 37 °C water bath. Aliquots (20 μL) were taken after 0, 0.5, 1, 1.5 and 4 hours and analyzed by HPLC.

Hydroxyapatite binding assay

65.2 mg of sodium phosphate and 870 mg of sodium chloride was dissolved in 100 mL PBS buffer solution and adjusted pH = 5.5 to afford buffer solution. 1 μM **BTM19-1**, **BTM19-2** and **BTM19-3** were respectively dissolved with 1 mL buffer solution and diluted 3 times for later use. 15 mg of HA was added to 1 mL of PDCs solution and incubated in 37 °C water bath. Aliquots (20 μL) were taken after 0, 10, 20, 40, and 80 minutes and analyzed by HPLC.

Enzymatic stability studies

222 mg of calcium chloride was dissolved in 1000 mL PBS buffer solution and adjusted pH = 7.4 to afford buffer solution. 5 mg of chymotrypsin was dissolved in 1 mL the above buffer solution and diluted 1000 times for later use. 1 μM **BTM19-1**, **BTM19-2** and **BTM19-3** were respectively dissolved with 1 mL buffer solution to prepare the stock solution. 1950 μL of the chymotrypsin solution was mixed with 50 μL of PDCs solution and incubated in 37 °C water bath. Aliquots (20 μL) were taken after 0, 0.5, 1, 2 and 4 hours and analysed by HPLC.

Cytotoxicity test

RAW264.7 cells were cultured in 96 well plates (1×10^5 mL^{-1}, 200 μL per well) for 48 hours co-cultured with designed PDCs and **M19** at the indicated concentration (0, 1.25, 2.5, 5 and 10 μM). Then, 10 μL of CCK-8 reagent was added and incubated for 4 hours in a 37 °C protected from light. The absorbance (OD) at 450 nm was recorded on the microplate reader. Cell survival rate = OD value of the experimental group/OD value of the blank control group; cytotoxic effect = 1 − cell survival rate.

In vitro osteoclast inhibition test

Murine osteoclast precursors from 8 week-old C57BL/6 male mice were cultured in 96 well plates (1×10^5 mL^{-1}, 200 μL per well) for 3 days co-cultured with 20 ng mL^{-1} murine CSF-1 and 300 ng mL^{-1} sRANKL with or without treatment of designed PDCs and **M19** at the indicated concentration (0, 1.25, 2.5, 5 and 10 μM). Then, the fixed cells were stained using tartrate-resistant acid phosphatase kit (Sigma). TRAP-positive multinucleated cells were observed by a microscope (OLYMPUS-BX53).

Conclusions

In summary, current efforts of PDCs were mainly focused on the targeted therapy of various malignant tumor, however, the research works of anti-osteoporotic PDCs have not been reported. These tailor-made thiomatrine derivative based bone-targeted PDCs for osteoporosis therapy developed in this work showed high cathepsin K sensitivity and affinity for hydroxyapatite *in vitro*. Besides, they not only performed satisfactory chemical and enzyme stability, but also lower cytotoxicity and similar osteoclasts inhibitory activity compared to the prototype drug. The optimal PDC **BTM19-2** was a suitable candidate for further evaluation in osteoporosis therapy research.

Author contributions

Shipeng He and Yong Wang designed the experiments; Jia Su and Chao Liu conducted the experiments; Honggang Hu revised the manuscript; Haohao Bai, Wei Cong, Fei Gao and Hua Tang analyzed the data.

Conflicts of interest

There are no conflicts to declare.

Acknowledgements

References

1 O. Johnell and J. A. Kanis, *Osteoporosis Int.*, 2006, **17**, 1726–1733.

2 M. Lorentzon, *J. Intern. Med.*, 2019, **285**, 381–394.

3 F. Salamanna, M. Maglio, V. Borsari, M. P. Landini and M. Fini, *Trends Endocrinol. Metab.*, 2021, **32**, 672–679.

4 T. D. Rachner, S. Khosla and L. C. Hofbauer, *Lancet*, 2011, **377**, 1276–1287.

5 T. Matsumoto and I. Endo, *J. Bone Miner. Metab.*, 2021, **39**, 91–105.

6 D. Bonn, *Lancet*, 2004, **363**, 786–787.

7 Y. J. Zhou, Y. J. Guo, X. L. Yang and Z. L. Ou, *J. Cancer*, 2018, **9**, 1357–1364.

8 B. Zhang, Z. Y. Liu, Y. Y. Li, Y. Luo, M. L. Liu, H. Y. Dong, Y. X. Wang, Y. Liu, P. T. Zhao, F. G. Jin and Z. C. Li, *Eur. J. Pharm. Sci.*, 2011, **44**, 573–579.

9 H. Hu, S. Wang, C. Zhang, L. Wang, L. Ding, J. Zhang and Q. Wu, *Bioorg. Med. Chem. Lett.*, 2010, **20**, 7537–7539.

10 L. M. Gao, Y. X. Han, Y. P. Wang, Y. H. Li, Y. Q. Shan, X. Li, Z. G. Peng, C. W. Bi, T. Zhang, N. N. Du, J. D. Jiang and D. Q. Song, *J. Med. Chem.*, 2011, **54**, 869–876.

11 H. Y. Gao, G. Y. Li, M. M. Lou, X. Y. Li, X. Y. Wei and J. H. Wang, *J. Inflammation*, 2012, **9**, 16.

12 X. Chen, X. Zhi, L. Cao, W. Weng, P. Pan, H. Hu, C. Liu, Q. Zhao, Q. Zhou, J. Cui and J. Su, *Cell Death Dis.*, 2017, **8**, e3037.

13 Y. Zou, M. Sarem, S. Xiang, H. Hu, W. Xu and V. P. Shastri, *BMC Cancer*, 2019, **19**, 949.

14 J. Li, J. Xu, Y. Lu, L. Qiu, W. Xu, B. Lu, Z. Hu, Z. Chu, Y. Chai and J. Zhang, *Molecules*, 2016, **21**, 649.

15 J. Xu, Y. Qi, W. H. Xu, Y. Liu, L. Qiu, K. Q. Wang, H. G. Hu, Z. G. He and J. P. Zhang, *Int. Immunopharmacol.*, 2016, **36**, 59–66.

16 H. Hirabayashi and J. Fujisaki, *Clin. Pharmacokinet.*, 2003, **42**, 1319–1330.

17 S. D. Chipman, F. B. Oldham, G. Pezzoni and J. W. Singer, *Int. J. Nanomed.*, 2006, **1**, 375–383.

18 E. S. Kim, D. Kim, S. Nyberg, A. Poma, D. Cecchin, S. A. Jain, K. A. Kim, Y. J. Shin, E. H. Kim, M. Kim, S. H. Baek, J. K. Kim, T. R. Doeppner, A. Ali, J. Redgrave, G. Battaglia, A. Majid and O. N. Bae, *Sci. Rep.*, 2020, **10**, 699.

19 D. Mahalingam, G. Wilding, S. Denmeade, J. Sarantopoulas, D. Cosgrove, J. Cetnar, N. Azad, J. Bruce, M. Kurman, V. E. Allgood and M. Carducci, *Br. J. Cancer*, 2016, **114**, 986–994.

20 T. B. Andersen, C. Q. López, T. Manczak, K. Martinez and H. T. Simonsen, *Molecules*, 2015, **20**, 6113–6127.

21 C. P. Leamon, M. A. Parker, I. R. Vlahov, L. C. Xu, J. A. Reddy, M. Vetzel and N. Douglas, *Bioconjugate Chem.*, 2002, **13**, 1200–1210.

22 H. Su, J. M. Koo and H. Cui, *J. Controlled Release*, 2015, **219**, 383–395.

23 W. Ma, A. G. Cheetham and H. Cui, *Nano Today*, 2016, **11**, 13–30.

24 D. D. Perrin, *Nature*, 1965, **208**, 787–788.

25 P. C. Bulman Page, J. P. G. Moore, I. Mansfield, M. J. McKenzie, W. B. Bowler and J. A. Gallagher, *Tetrahedron*, 2001, **57**, 1837–1847.

26 G. Caselli, M. Mantovanini, C. A. Gandolfi, M. Allegretti, S. Fiorentino, L. Pellegrini, G. Melillo, R. Bertini, W. Sabbatini, R. Anacardio, G. Clavenna, G. Sciortino and A. Teti, *J. Bone Miner. Res.*, 1997, **12**, 972–981.

27 T. M. Willson, B. R. Henke, T. M. Momtahen, P. L. Myers, E. E. Sugg, R. J. Unwalla, D. K. Croom, R. W. Dougherty, M. K. Grizzle, M. F. Johnson, K. L. Queen, T. J. Rimele, J. D. Yingling and M. K. James, *J. Med. Chem.*, 1996, **39**, 3030–3034.

28 S. Kasugai, R. Fujisawa, Y. Waki, K. Miyamoto and K. Ohya, *J. Bone Miner. Res.*, 2000, **15**, 936–943.

29 Y. Sun, X. Ye, M. Cai, X. Liu, J. Xiao, C. Zhang, Y. Wang, L. Yang, J. Liu, S. Li, C. Kang, B. Zhang, Q. Zhang, Z. Wang, A. Hong and X. Wang, *ACS Nano*, 2016, **10**, 5759–5768.

30 G. S. Nowakowski, M. S. Dooner, H. M. Valinski, A. M. Mihaliak, P. J. Quesenberry and P. S. Becker, *Stem Cells*, 2004, **22**, 1030–1038.

31 H. Wu, G. Zhang, B. S. Guo, T. Tao, G. Li, K. M. Lee, L. K. Hung and L. Qin, *Bone*, 2010, **47**, S413–S414.

32 T. A. Stone and C. M. Deber, *Biochim. Biophys. Acta, Biomembr.*, 2017, **1859**, 577–585.

33 V. Everts, W. Korper, K. A. Hoeben, I. D. Jansen, D. Bromme, K. B. Cleutjens, S. Heeneman, C. Peters, T. Reinheckel, P. Saftig and W. Beertsen, *J. Bone Miner. Res.*, 2006, **21**, 1399–1408.

34 V. Everts, J. M. Delaissé, W. Korper, D. C. Jansen, W. Tigchelaar-Gutter, P. Saftig and W. Beertsen, *J. Bone Miner. Res.*, 2002, **17**, 77–90.

35 C. W. Hsu, R. M. Olabisi, E. A. Olmsted-Davis, A. R. Davis and J. L. West, *J. Biomed. Mater. Res., Part A*, 2011, **98**, 53–62.

36 K. Chang and F. Jaffer, *J. Nucl. Cardiol.*, 2008, **15**, 417–428.

37 M. J. Bossard, T. A. Tomaszek, S. K. Thompson, B. Y. Amegadzie, C. R. Hanning, C. Jones, J. T. Kurdyla, D. E. McNulty, F. H. Drake, M. Gowen and M. A. Levy, *J. Biol. Chem.*, 1996, **271**, 12517–12524.

38 K. Date, H. Sakagami and K. Yura, *Sci. Rep.*, 2021, **11**, 12023.

39 K. Hochdörffer, K. Abu Ajaj, C. Schäfer-Obodozie and F. Kratz, *J. Med. Chem.*, 2012, **55**, 7502–7515.